6th International Symposium on Three-Dimensional Electromagnetics
Berkeley, California, March 28–30, 2017

3D MT and CSEM modeling with multi-resolution grid

M. Cherevatova[1], G. D. Egbert[2], M. Yu. Smirnov[3] and M. Becken[1]
[1]University of Muenster, Germany
[2]Oregon State University, USA
[3]Luleå University of Technology, Sweden

Summary

We present 3D forward modeling based on a multi-resolution grid, which allows calculation of the electromagnetic field for magnetotelluric and controlled source applications. The finer grid discretization is required near the source location to accurately model rapidly varying electromagnetic fields, near-surface anomalies, bathymetry and topography. On the other hand, the EM field propagates in a diffusive manner and can be sufficiently well described on a grid that becomes gradually coarser with depth. The multi-resolution grid allows us to significantly decrease the number of degrees of freedom and hence improve on the computational efficiency without compromising the accuracy of the solution. In our implementation, the multi-resolution grid represents a vertical stack of sub-grids. We allow grid refinement in only horizontal directions, using quadtree scheme (which can be extended to octree as well). Each sub-grid represents a standard staggered grid. Therefore, operators and functions already developed for a simpler standard structured grid can be applied for each sub-grid. The major difficulty lies in the treatment of the hanging edges (and nodes) on the interfaces between adjacent sub-grids of different resolution. We considered several approaches to defining a set of active edges on the interface. By active we imply edges, being used for calculation of the curl-curl operator on the full multi-resolution grid. The case, where active edges are taken from the coarser sub-grid has substantial advantages (accurate solution and symmetric curl-curl operator) over the cases with active edges taken from the finer sub-grid, or interpolation. The approach is implemented within the object oriented framework ModEMM, in Matlab.

Keywords: forward modeling, MT, CSEM, multi-resolution grid

Introduction

The novel multi-resolution approach was initially developed for magnetotelluric (MT) applications. Later, it was extended to include controlled source (CS) modeling. The development is done within the framework of the object-oriented code in Matlab (ModEMM) specifically created for testing purposes (Egbert, Smirnov, & Cherevatova, 2017). The code consists of basic modules, allowing for modeling of the electromagnetic (EM) field in all three dimensions on a staggered grid. Further extension of the code was done to include anisotropy, spherical coordinates, multi-grid solver and induced polarization. The object oriented approach makes it easy to add new methods to the code by simple extension of availbale functionality. We develop modeling within the finite difference (FD) approximation on a staggered grid (SG). The multi-resolution (MR) grid represents a set of sub-grids of different discretization. Each sub-grid is a standard staggered grid. The forward problem is solved for electric fields, defined on edges of the grid. Therefore, reducing the number of edges, we reduce the number of equations to be solved, with benefits in terms of computational costs, as result. To solve the CSEM problem we follow the secondary field approach. This requires calculation of background field on each edge of the modeling domain. As we reduce the number of edges with MR grid, we can benefit on computational time for the 1D background field as well. The system of equations $\mathbf{Ax}=\mathbf{b}$ can be solved for $\mathbf{x}$ with a direct or an iterative solver. Iterative solvers require less memory and computation time than direct ones, however they depend on proper preconditioning. Direct-solution techniques on the other hand provide better numerical accuracyand are beneficial for controlled source. Direct solvers at the same time are limited by the size of the model, which significantly increases memory requirements. Our MR approach allows us to use finer horizontal resolution at the surface keeping those requirements within the reasonable limits. An example of a simple multi-resolution grid is shown in Fig. 1. Our approach is similar to the octree scheme of Haber and Heldmann (2007) and Horesh and Haber (2011), where each grid cell can be subdivided in halfs in each direction. However, we allow grid refinement

in only the horizontal directions, using a quadtree scheme (Finkel & Bentley, 1974). We start to derive the multi-resolution grid from the fine grid of the dimension $N_x \times N_y \times N_z$, subdividing it into N_{sg} sub-grids. Each sub-grid i has $N_z(i)$ vertical layers. The coarseness of each sub-grid is thus defined by the parameter $Cs(i), i = 1, ..., N_{sg}$, which can take the values of 0, 1, 2, 3, etc. Therefore, horizontal grid dimensions for sub-grid i are then calculated as $N_x/2^{Cs(i)} \times N_y/2^{Cs(i)}$. Thus, the MR grid is fully defined (in terms of a base fine grid) by two parameters $[Cs(i),\ N_z(i)]$.

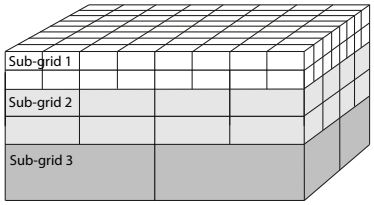

Figure 1: Example of the multi-resolution grid composed of three sub-grids. Coarseness [Cs, N_z] = [0,2; 1,2; 2,1].

Implementation

We solve a system of partial differential equations (PDEs) in terms of the electric field. At the frequencies used, the displacement currents can be neglected and a time dependence of $e^{(i\omega t)}$ is assumed. With the SG approach of Yee (1966) the discretized electric field vector components $\mathbf{e}$ are defined on cell edges, and the magnetic field components are defined on cell faces. Therefore, on this grid the discretized PDEs can be expressed as

$$[\mathbf{C}^\dagger\mathbf{C} + \mathbf{diag}(i\omega\mu\sigma(\mathbf{m}))]\mathbf{e} = \mathbf{j}_s, \tag{1}$$

with the tangential electric field components specified on the boundaries. Here, $\mathbf{j}_s$ defines source currents (zero for the MT problem), $\mathbf{C}$ is the discrete approximation of the curl operator (mapping cell edges to cell faces), and $\mathbf{C}^\dagger$ is the adjoint of the discrete curl operator, which maps cell faces to the vector of cell edges. Finally, $\sigma(\mathbf{m})$ represents the mapping of the model parameters $\mathbf{m}$ (conductivity) defined on cell edges, where the electric field components are defined. For the MT case, the system of eqs. 1 is solved for the total field $\mathbf{e}$, while the secondary field approach is used for CS problem $\mathbf{e} = \mathbf{e}_s$. The source term on the right-hand side is then defined as $\mathbf{j}_s = -i\omega\mu(\sigma(\mathbf{m}) - \sigma_b(\mathbf{m}))\mathbf{e}_b$, where σ_b is the background conductivity. The background field $\mathbf{e}_b$ is computed analytically for a homogeneous background model or for a 1D horizontally layered model given at the source point (Wait, 1982). In order to improve computational efficiency of the iterative solver we perform the divergence correction of the solution. The discrete curl operator $\mathbf{C}$ in eq. (1) can be decomposed into simpler matrices, defining the topology of the curl operator on the SG, and diagonal matrices of metric elements. The topology matrix $\mathbf{T}$ corresponds to the discrete curl operator defined on an uniform unit-cell grid, with all non-zero elements ± 1. Diagonal matrices of metric elements needed to define the curl on an arbitrary SG include edge length ($\mathbf{L}_E$),face area ($\mathbf{A}_F$) and cell volume ($\mathbf{V}_C$). Corresponding elements are also needed for the dual grid, based on dual edges which connect cell centers ($\mathbf{L}_{\tilde{E}}$, $\mathbf{A}_{\tilde{F}}$, and $\mathbf{V}_{\tilde{C}}$). Then from Stokes' theorem it is readily seen that the curl operator on a general staggered grid can be written

$$\mathbf{C} = \mathbf{A}_F^{-1}\mathbf{T}\mathbf{L}_E. \tag{2}$$

Similarly, the adjoint curl (mapping the vector field defined on faces back to the edges) can be given in terms of the transpose of the curl topology matrix, and dual metric elements, as

$$\mathbf{C}^\dagger = \mathbf{A}_{\tilde{F}}^{-1}\mathbf{T}^T\mathbf{L}_{\tilde{E}}. \tag{3}$$

For a general (non-uniform) grid the discrete curl-curl operator formed from the matrices defined in (2) and (3) is not symmetric. However, multiplying by the edge volume $\mathbf{A}_{\tilde{F}}\mathbf{L}_E$ yields

$$\mathbf{A}_{\tilde{F}}\mathbf{L}_E\mathbf{C}^\dagger\mathbf{C} = \mathbf{L}_E\mathbf{T}^T\mathbf{L}_{\tilde{E}}\mathbf{A}_F^{-1}\mathbf{T}\mathbf{L}_E, \tag{4}$$

which is symmetric. The same approach is used to define the discrete operators needed for the divergence correction, starting from $\mathbf{T}$, the topology matrix for the gradient.

As noted already, the MR grid is represented as a vertical stack of fixed-resolution staggered grids. This allows us to construct discrete curl operators for the MR grid using the FD SG operators. To be explicit, let $\mathbf{e}_{full}$ be the full vector consisting of all edges in each sub-grid, stacked together, and define $\mathbf{T}_{full}$ as the block diagonal matrix, with each block $\mathbf{T}_i$ being the standard SG curl (topology) operator for sub-grids $i = 1, ..., N_{sg}$.

On the interface between adjacent sub-grids we will have overlapping edges (and faces) from finer and coarser sub-grids. To make the problem well defined we should choose edges (and faces) from one of the adjacent sub-grids (either fine or coarse is possible) to be "active", and then eliminate the inactive (redundant) interface components from the other grid. Values on inactive edges, which are needed for computation of the curl must then be derived (through

interpolation or averaging) from values on the active edges.

At first blush the most natural approach (Haber & Heldmann, 2007) is to take the fine-grid edges as active, and eliminate the coarse-grid components on the interface. In this case the definition of the curl operator $\mathbf{C}$ is clear: every face is bounded by exactly four edges, and (2) provides a physically sensible discrete approximation to this operator. However, when active edges and faces on interfaces are taken from the fine grid an appropriate definition of the adjoint curl (needed to compute the curl of the magnetic fields defined on faces, mapping back to edges) is not simple. An edge which subdivides a coarse face only bounds 3 fine-grid faces, so the corresponding row of $\mathbf{T}^T$ only includes these 3 faces in the computation of the curl around this "hanging" edge. Thus, Eq. (3) does not define a physically reasonable approximation to the curl in the vicinity of the interface, and in the curl-curl operator the "paddle wheel" for such a hanging edge will be incomplete.

One way to deal with this problem (Horesh & Haber, 2011) is to interpolate from the coarse-grid faces in the layer below to the missing, or "ghost", fine-grid face needed to complete the adjoint curl stencil. This approach, which we also implement, will result in greater accuracy (Horesh & Haber, 2011), but complicates implementation of the adjoint curl, which can no longer be given simply in terms of the transpose of $\mathbf{C}$ as in (3). This modification of the adjoint curl breaks the symmetry of the volume weighted curl-curl operator (4), with some potential impacts on iterative solver performance, and additional complications in sensitivity calculations. An alternative definition of the active edges, and of the basic curl operator $\mathbf{C}$, allows a physically sensible adjoint curl to be defined in terms of the matrix transpose, thus retaining symmetry in the discrete curl-curl operator.

In the alternative approach we take the coarse-grid edges on the interface to be active, and omit all fine-grid edges. Active faces in the interface layer are similarly taken from the coarse grid. Now the (vertical) x and y-faces in the fine grid that abut the interface ("hanging faces") only have three bounding (fine-grid) edges. To compute the curl on these faces we thus must first "fill in" the omitted fine-grid edges, by interpolation from the active coarse-grid edges. Allowing for the factor of 2 difference in length of the fine and coarse grid edges, omitted fine edges that subdivide a coarse edge (c_1), should be set as $c_1/2$. For edges which are not bounded by any coarse edge we can interpolate between neighbouring coarse-grid edges (c_1 and c_2) on either side, and again taking account of the difference in fine and coarse grid edge length, set $(c_1 + c_2)/4$.

With this second approach there are no hanging edges on the interface layer, and defining the adjoint curl as in (3) is still physically sensible. Considering the dual-grid edge lengths and face areas (which differ by a factor of two between the coarse and fine grid), Eq. (3) can be seen to define a physically sensible discrete approximation to the adjoint curl. The only difference relative to the usual "paddle wheeel" for a uniform grid is that multiple faces above the interface in the fine grid are averaged in the curl computation. Similar considerations apply to the gradient and divergence operators required for the divergence correction.

Results

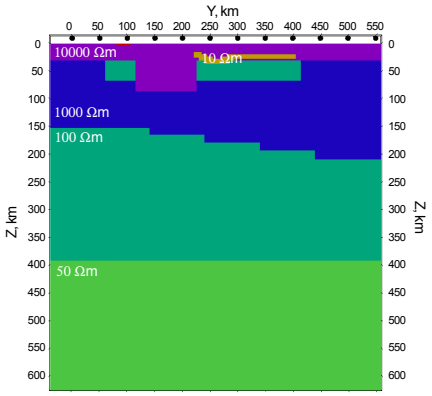

Figure 2: Synthetic 3D model, cross-section view for profile.

We compare accuracy and speed of the three variants discussed above: active edges, faces, and nodes on the interfaces taken from the finer grid (MR1) and from the coarser grid (MR3) with adjoint operators computed simply using matrix transpose, and (MR2) with adjoint operators computed by interpolation. Approaches MR1 and MR3 result in symmetric systems of equations (after weighting), while MR2 does not. A comparison of the 3D MT MR, SG solutions with the 1D response for the layered model reveals a great accuracy of the MR2 and MR3 cases. The relative error on the apparent resistivity for these MR cases and SG is within the numercal errors of 10^{-8} and absolute differences for phase is 10^{-7} degrees. The MR1 case differs significantly from 1D result with 1.5% for apparent resistivity and up to 0.2^o for phase of the impedance tensor.

In order to estimate the accuracy of the 3D iterative solver we consider a realistic 3D synthetic example, based on the real model obtained from 3D inversion

of the MaSca data set from north-west Fennoscandia (Cherevatova et al., 2015). The model is uniformly discretized into 128 cells in the x and y directions and 80 cells in the z direction (plus 12 air layers), resulting in 1,507,328 model parameters for the staggered grid. The multi-resolution grid consists of seven sub-grids with four coarsening levels $[C_z, N_z] = [2, 4; 1, 4; 0, 41; 1, 14; 2, 9; 3, 5; 4, 15]$, resulting in 761,024 model parameters. The solution converged to the tolerance of 10^{-9}.

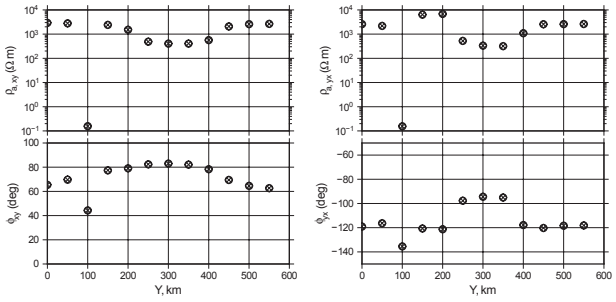

Figure 3: Apparent resistivity and phase of the impedance tensor at period of 10 s. Crosses – SG, diamonds – MR2 and circles – MR3

In Fig. 3 the apparent resistivity and phase of the impedance tensor are shown for profile, crossing structures presented in Fig. 2. We compare two multi-resolution cases MR2 (diamonds) and MR3 (circles) with the staggered grid SG (crosses), which we consider as a reference solution. As it can be seen, MT responses agree well for all approaches, with the relative error of 0.2% for apparent resistivity and the phase difference of 0.1^o. Despite of the same accuracy in the solution between MR2 and MR3 cases, MR3 has greater advantage to preserve the symmetry of the "curl-curl" operator.

The speed-up of the multi-resoluton solver grows with the number of the unknowns. In particular, MR is two times faster than SG for smaller model "64" and 5 times faster for large model "256".

Conclusions

The multi-resolution forward solver allows computations to be speed up by several times; the scheme also has smaller memory requirements. Therefore, inversion based on the multi-resolution grid forward solver might provide significant computational advantages, and also allows for greater flexibility in terms of model discretization and better resolution of near-surface features, topography, bathymetry and source. To maintain efficiency of iterative solvers, and to simplify adjoint sensitivity calculations for inversion applications it is desirable to preserve symmetry of discretized operators. We considered three approaches to discretization of the forward operators on the interface between adjacent sub-grids. Various tests with the synthetic 1D and 3D model, which will be presented, shows that the MR3 approach (active interface edges, nodes and faces taken from the coarser grid) allows for more accurate solution with the advantage of being symmetric. We considered only quadtree scheme, however, hanging edges, nodes and faces can be extended to a full octree with variable horizontal as well as vertical refinement.

REFERENCES

Cherevatova, M., Smirnov, M., Korja, T., Pedersen, L., Ebbing, J., Gradmann, S., et al. (2015). Electrical conductivity structure of north-west Fennoscandia from three-dimensional inversion of magnetotelluric data. *Tectonophysics*, *653*, 20 - 32.

Egbert, G., Smirnov, M., & Cherevatova, M. (2017). *Development of Flexible Object Oriented Matlab Codes for 3D EM Modeling.*

Finkel, R., & Bentley, J. (1974). Quad trees a data structure for retrieval on composite keys. *Acta Informatica*, *4*, 1-9.

Haber, E., & Heldmann, S. (2007). An octree multigrid method for quasi-static Maxwell's equations with highly discontinuous coefficients. *Journal of Computational Physics*, *223*, 783-796.

Horesh, L., & Haber, E. (2011). A Second Order Discretization of Maxwell's Equations in the Quasi-Static Regime on Octree Grids. *SIAM J. on Scientific Computing*, *33*, 2805-2822.

Wait, J. R. (1982). In J. R. Wait (Ed.), *Geo-electromagnetism.* Academic Press.

Yee, K. S. (1966). Numerical Solution of Initial Boundary Value Problems Involving Maxwell's Equations in Isotropic Media. *IEEE. Trans. Anten. Propag.*, *14*(3), 302–307.